A flexible nonlinear Resonance Driving Term based Correction Algorithm with feed-down

J. Dilly, R. Tomás

Summary

The optics in the insertion regions of the LHC and its upgrade project the High Luminosity LHC are very sensitive to local magnetic errors, due to the extremely high beta-functions present. In collision optics, the non-zero closed orbit in the same region leads to a "feed-down" of high-order errors to lower orders, causing additional effects detrimental to beam lifetime. An extension to the proven method for correcting these errors by locally suppressing resonance driving terms has been undertaken, not only taking this feed-down into account, but also adding the possibility of utilizing it such that the powering of higher-order correctors will compensate for lower order errors. Existing correction schemes have also operated on the assumption of symmetric beta-functions of the optics in the two rings. As this assumption can fail for a multitude of reasons, such as inherently asymmetric optics and unevenly distributed errors, an extension of this correction scheme has been developed removing the need for symmetry by operating on the two separate optics of the beams at the same time. In contrast to earlier implementations, the resonance driving terms to correct can also flexibly changed. The mathematical background as well as the implementation of this new extension are presented in this note.

Contents

1 Motivation

The sensitivity of accelerator beam optics to magnetic errors depends directly on the β-function, which is highest in the Insertion Regions (IR) around the Interaction Points (IP) with the lowest β^* (the value of the β-function at the location of the IP). Hence, correcting the non-linear magnetic errors in these regions has been of significant importance in optimizing the LHC machine performance [1, 2, 3, 4, 5, 6].

During the design phase of the LHC, it was envisaged to make use of the magnetic measurement data of the LHC magnets [7, 8, 9] to simulate the machine in MAD-X [10] and calculate the errors [11]. While it became clear that the accuracy of the magnetic model was not sufficient to calculate corrections to be implemented in the LHC [12], it has nevertheless been a useful tool for the estimation of linear and non-linear effects [5, 12, 13, 14, 15].

Installation of stronger magnets in the IR and the decrease of β^* in operation in the High Luminosity upgrade of the LHC (HL-LHC) [16, 17], is foreseen to result in even tighter constraints on residual errors.

At the same time, the influence of feed-down has been observed and investigated in the IRs of the LHC as well, where the crossing-angle scheme of the collision optics creates a large orbit bump. For both, LHC and HL-LHC the need for corrections of this feed-down has been established [2, 4, 5, 6, 12, 18, 19, 20].

To estimate the powering of the corrector magnets, a local correction scheme based on the Resonance Driving Terms (RDTs) in the IRs has been utilized [11]. Up to now, the implementation of this scheme calculated the correction based on a single input optics, for either Beam 1 or Beam 2, and made use of symmetries between the beams to optimize the correction for both. Cases will occur in which this symmetry does not hold, e.g. through the introduction of feed-down, or the use of inherently asymmetric optics. An example for the latter are flat optics [21, 22], in which β^* in the two transversal planes no longer has identical values. These optics allow for a more distributed radiation deposition in the LHC magnets as well as an increase in luminosity [22]. Their feasibility has been studied during machine developments in the LHC [23] and preliminary analysis regarding their influence on corrections and amplitude detuning has been conducted [24]. A new and flexible version of the correction principle has been implemented [25], taking up to two optics into account and hence not relying on symmetry assumptions, allowing to target RDTs freely, as well as including feed-down into the calculations. The implementation allows for the feed-down from higher orders to the RDT to be corrected, as well as using the feed-down from higher order corrector magnets to correct for lower order errors. Theoretical background and the implementation details of this algorithm are presented in this report.

2 Background

2.1 Nonlinear Correctors

Due to the high β-functions around the experimental IPs, the optics of the LHC and HL-LHC are very sensitive to field imperfections in the surrounding triplets. To compensate for these errors locally, both sides of the LHC IRs hosting experiments (ATLAS in IR1, ALICE in IR2, CMS in IR5 and LHCb in IR8) are equipped with linear and non-linear corrector

packages. As shown in the schematics of Figs. 1 and 2, these packages are located within the common aperture region of the machines, between Q3 and the separation dipoles D1, and hence contain common magnets for the two beams. Any correction should therefore take the optics of both beams into account.

In the experimental IRs of the LHC and in HL-LHC IR2 and IR8, nonlinear correctors for skew and normal sextupoles (a_3, b_3), skew and normal octupoles (a_4, b_4) and normal dodecapoles (b_6) are available. In IR1 and IR5 in the HL-LHC on the other hand, the corrector package will be upgraded to also include skew and normal decapoles (a_5, b_5) as well as skew dodecapoles (a_6) and offer therefore a wider range of field errors to correct, to account for the increase in the β-function in this high-performance machine [17, 26, 20].

The correctors MCSSX.3L2, MCOX.3L2, MCOSX.3L2, MCOSX.3L1 have not been present in LHC Run 2 and Run 3. These are the skew sextupole, octupole and skew ocupole correctors left of IP2 (possibly due to a hit from a pilot beam), as well as the skew octupole corrector left of IP1 (probably due to powering issues). Their absence is already reflected in the lattice used for simulations [27].
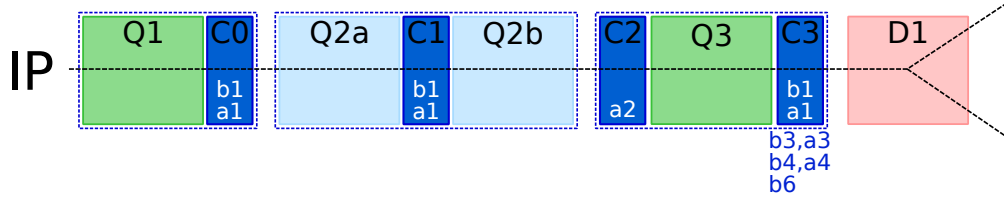
Figure 1: Schematic of the right hand side of a LHC IR region and HL-LHC IR2 and IR8. Q1, Q2a/b and Q3 are the triplet quadrupoles. C0-C3 show the corrector packages with the field order to be corrected indicated. The blue lines mark common cryostats. The non-linear corrector package is included with the orbit correctors in C3.
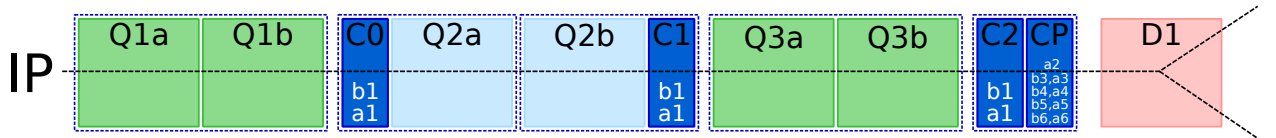
Figure 2: Schematic of the right hand side of HL-LHC IR1 and IR5. Q1a/b, Q2a/b and Q3a/b are the triplet quadrupoles. C0, C1, C2 and CP show the corrector packages with the field order to be corrected indicated. The blue lines mark common cryostats.

2.2 Resonance Driving Terms

The transformation of the phase-space coordinates of a particle propagating through a circular accelerator can be described by means of maps, each describing the transformation generated by an element of the machine. These maps are symplectic, i.e. they preserve phase-space volume, and can be combined, describing the propagation through multiple parts of the accelerator [28], for example one complete turn.

Using Lie-Algebra notation [28, 29]

$$:f := \sum_{z=x,y} \frac{\partial f}{\partial z}\frac{\partial}{\partial p_z} - \frac{\partial f}{\partial p_z}\frac{\partial}{\partial z} \qquad (1)$$

a linear one turn map $\mathcal{M}$ can be transformed into a rotation R, its normal form:

$$\mathcal{M} = e^{:h:}R . \qquad (2)$$

In case of nonlinear elements present in the machine, the transformation becomes [30]:

$$\mathcal{M} = e^{-:F:}\, e^{:h:} R\, e^{:F:} . \qquad (3)$$

This transformation depends on the location s at which the one-turn-map is calculated. Truncating the exponential series at first order, it can be shown [31] that

$$h(s) = \sum_{jklm} h_{jklm}(s)\, (2J_x)^{\frac{j+k}{2}} (2J_y)^{\frac{l+m}{2}} e^{-i[(j-k)(\phi_x(s)+\phi_{x,0})+(l-m)(\phi_y(s)+\phi_{y,0})]} , \qquad (4)$$

with $\phi_z(s)$ being the phase in plane $z = x, y$ at s and $\phi_{z,0}$ the initial phase of the particle at injection. J is the action, i.e. the invariant of (linear) motion [32] and h_{jklm} are the Hamiltonian coefficients [31], which are defined by all sources around the ring of multipole order $n = j + k + l + m$ (see Section 2.3).

The contribution h_{jklm} from multipole sources of order $n \geq 2$ to the hamiltonian is given in [33] Eq. (3.11) as

$$h_{jklm}(s) = -\Re\left[\frac{i^{l+m}}{j!\,k!\,l!\,m!\,2^{j+k+l+m}} \beta_x(s)^{\frac{j+k}{2}} \beta_y(s)^{\frac{l+m}{2}} \left(K_n(s) + iJ_n(s)\right) \right] . \qquad (5)$$

$K_n(s)$ and $J_n(s)$ are the magnetic field strengths of order n at location s of normal and skew fields respectively. In this note, we use the convention of **starting the index n at 1, representing dipole fields** ($n = 2$ for quadrupole fields, etc.)

Similarly to $h(s)$, $F(s)$ is calculated as

$$F(s) = \sum_{jklm} f_{jklm}(s)(2I_x)^{\frac{j+k}{2}} (2I_y)^{\frac{l+m}{2}} e^{-i[(j-k)(\psi_x(s)+\psi_{x,0})+(l-m)(\psi_y(s)+\psi_{y,0})]} , \qquad (6)$$

with I_z and ψ_z being the action and angle coordinates of the nonlinear motion (called canonical coordinates of the normal form). The generating terms f_{jklm} of F are the so called Resonance Driving Terms (RDTs) and it is shown in [30] (also given in [33] Eq. (3.15)) that their relation to the hamiltonian terms is

$$f_{jklm}(s) = \oint_{\text{Ring}} \frac{h_{jklm}(s')\, (2J_x)^{\frac{j+k}{2}} (2J_y)^{\frac{l+m}{2}} e^{-i[(j-k)\cdot\Delta\phi_x(s,s')+(l-m)\cdot\Delta\phi_y(s,s')]}}{1 - e^{-i2\pi[(j-k)Q_x+(l-m)Q_y]}}\, ds' . \qquad (7)$$

$\Delta\phi_z(s, s')$ is the phase advance in plane $z = x, y$ between s and s', while Q_z are the horizontal and vertical tunes, i.e. the number of betatron oscillations per turn.

5

In case of the condition

$$(j - k) \cdot Q_x + (l - m) \cdot Q_y = 2\pi \cdot p \tag{8}$$

being fulfilled for $p \in \mathbb{Z}$, f_{jklm} diverges, if there are sources present for that order. In this case the system is in a resonant state, and hence instable. The behaviour of the instability as the systems approaches the resonance condition therefore depends on the strength of the multipole sources present in the machine. Resonances labeled (n_x, n_y) are driven by all terms $n_x = j - k$ and $n_y = l - m$.

For each resonance (n_x, n_y) there is a line in the spectrum obtained by turn-by-turn beam position measurements, which can be found at $-(n_x - 1) \cdot Q_x - n_y \cdot Q_y$ (label: $(-n_x + 1, -n_y)$) in the spectrum of the horizontal plane and $-n_x \cdot Q_x - (n_y - 1) \cdot Q_y$ (label: $(-n_x, -n_y + 1)$) in the spectrum of the vertical plane [33]. The amplitude of these lines is proportional to $|f_{jklm}(s)|$ [33], the terms are therefore easily accessible from measurements [34, 31, 35, 36, 37].

The h_{jklm}, and therefore f_{jklm}, are constant along s until a multipole source of corresponding order is encountered, at whose location its value jumps, which makes them very well suited as local observables [35]. The correction algorithm presented here is based on locally minimizing the RDTs in the IR as shown in the next section.

2.3 Correction Principle

In this section the correction principle as implemented in the flexible correction algorithm v1.0.0 in [25] is described. The algorithm follows the simplifications of Eqs. (5) and (7) as outlined in [11]:

- Only the contribution from elements in one IR to the RDTs are minimized. The integral in Eq. (7) includes therefore only IR elements.
- Constant coefficients of Eq. (7) are ignored, i.e. the numerator and actions as well as the coefficients depending only on j, k, l, m and any signs, as they are not needed for minimization, .
- The phase of one side of the IR is approximately constant, as $\Delta\Phi(a, b) = \int\limits_a^b \frac{1}{\beta(s)} ds$ and $\beta(s)$ being very large in the triplets.
- The phase-advance between the left and right side of the IP is π.
- The RDT is evaluated locally at the entrance of the IR.

With these approximations Eq. (7) becomes an *effective* RDT to minimize:

$$f_{jklm}^{\mathrm{IR}} = \int\limits_{\mathrm{IR}} \Re\left[i^{l+m}\left(K_n(s) + iJ_n(s)\right)\right] \beta_x(s)^{\frac{j+k}{2}} \beta_y(s)^{\frac{l+m}{2}} e^{i\pi n\theta(s - s_{\mathrm{IP}})} ds \;, \tag{9}$$

with $\theta(x)$ being the heaviside step function and s_{IP} the location of the IP within the IR. The n in the exponent replaces $j - k + l - m = n - 2k - 2l$, as for even (odd) n, this value will also be even (odd), independent of the particular choices for j, k, l, m.

The main concept of the correction is then to find the $K_n(s)$ and $J_n(s)$ of the corrector magnets, that minimize a set of given f_{jklm}^{IR} based on given optics.

As there are usually two correctors per multipole field available (one on each side of the IP), two combinations of $l+m$ and $j+k$ (the exponents of the β function) can be corrected. As the correctors are responsible for the correction of both beams, the exponents need to be chosen such that the correction is valid for both beams, which means that only a single RDT per beam can be corrected unless the symmetry of the optics can be used to correct two RDTs (see Section 2.3.2).

In the LHC a_3, b_3, a_4, b_4 and b_6 correctors are available, in the HL-LHC additionally a_5, b_5 and a_6.

2.3.1 Equation System

In our simulations, the input to the correction algorithm will be the output of `TWISS` and `ESAVE` functions from `MAD-X` [38]. These are tables in which $K_n(s)$ and $J_n(s)$ are not continuous functions, but given as already integrated values K_nL_w, J_nL_w (`K`$_{n-1}$`L`, `K`$_{n-1}$`SL` in the terminology of `MAD-X`) for each element w. Values for the longitudinal position $s_w, \beta_{x,w}, \beta_{x,w}$ and the transversal orbit x_w, y_w, which will be important when calculating feed-down (see below), are also provided.

To assure aa accurate estimate for the integral in Eq. (9), the lattice should be *sliced* in `MAD-X`, i.e. all magnets are approximated by single kicks surrounded by drift-spaces. Long magnets should be cut into multiple of these slices to increase accuracy. Corrector magnets on the other hand, which are in any case short compared to e.g. dipoles, can be represented by a single slice.

In this thin-lens approximation, Eq. (9) transforms into a sum over all elements (slices) w in the IR, which needs to be set to zero to suppress the RDT:

$$f_{jklm}^{\mathrm{IR}} = \sum_{w \in \mathrm{IR}} \Re \left[i^{l+m} \left(K_nL_w + iJ_nL_w \right) \right] \beta_{x,w}^{\frac{j+k}{2}} \beta_{y,w}^{\frac{l+m}{2}} e^{i\pi n\theta(s_w - s_{\mathrm{IP}})} \overset{!}{=} 0 . \tag{10}$$

Splitting the elements into corrector elements $\mathcal{C}$ and non-corrector elements IR $\setminus \mathcal{C}$, Eq. (10) transforms into:

$$\begin{aligned} &\sum_{w \in \mathcal{C}} \Re \left[i^{l+m} \left(K_nL_w + iJ_nL_w \right) \right] \beta_{x,w}^{\frac{j+k}{2}} \beta_{y,w}^{\frac{l+m}{2}} e^{i\pi n\theta(s_w - s_{\mathrm{IP}})} \\ &= - \sum_{w \in \mathrm{IR} \setminus \mathcal{C}} \Re \left[i^{l+m} \left(K_nL_w + iJ_nL_w \right) \right] \beta_{x,w}^{\frac{j+k}{2}} \beta_{y,w}^{\frac{l+m}{2}} e^{i\pi n\theta(s_w - s_{\mathrm{IP}})} \end{aligned} , \tag{11}$$

It is important to note, that each corrector is defined by either K_nL or J_nL, so that per order n and orientation (normal, skew) only a limited set of correctors is left. Normally there are two of these correctors in the LHC/HL-LHC, i.e. one per IP side, and $\mathcal{C} = \{cl, cr\}$, a left (cl) and a right (cr) corrector element. Defining the sum over IR$\setminus\mathcal{C}$ in Eq. (11) as I_{jklm} and

$$\begin{aligned} b_{jklm}^{(cl)} &= i^{l+m} \beta_{x,cl}^{\frac{j+k}{2}} \beta_{y,cl}^{\frac{l+m}{2}} \\ b_{jklm}^{(cr)} &= (-1)^n \, i^{l+m} \beta_{x,cr}^{\frac{j+k}{2}} \beta_{y,cl}^{\frac{l+m}{2}} , \end{aligned} \tag{12}$$

Eq. (11) can be split into a two equation system

$$
\begin{pmatrix} b_{jklm}^{(cl)} & b_{jklm}^{(cr)} \end{pmatrix} \begin{pmatrix} K_n L_{cl} \\ K_n L_{cr} \end{pmatrix} = -I_{jklm} \qquad \text{if } l+m \text{ even,}
$$
$$
\begin{pmatrix} i\, b_{jklm}^{(cl)} & i\, b_{jklm}^{(cr)} \end{pmatrix} \begin{pmatrix} J_n L_{cl} \\ J_n L_{cr} \end{pmatrix} = -I_{jklm} \qquad \text{if } l+m \text{ odd,}
$$

(13)

which can be easily extended to include multiple RDTs, e.g.:

$$
\begin{pmatrix} b_{jklm}^{(cl)} & b_{jklm}^{(cr)} \\ b_{j'k'l'm'}^{(cl)} & b_{j'k'l'm'}^{(cr)} \end{pmatrix} \begin{pmatrix} K_n L_{cl} \\ K_n L_{cr} \end{pmatrix} = - \begin{pmatrix} I_{jklm} \\ I_{j'k'l'm'} \end{pmatrix}
$$

(14)

with $j + k + l + m = j' + k' + l' + m' = n$ and $l + m$ and $l' + m'$ both even. These linear equation systems can be solved or optimized for $K_n L_{cl,cr}$ or $J_n L_{cl,cr}$ by standard algorithms.

2.3.2 Dual Optics

(a) $\beta^* = 15\,\text{cm}$ round optics (b) $\beta^* = 7.5\,\text{cm}/30\,\text{cm}$ flat optics
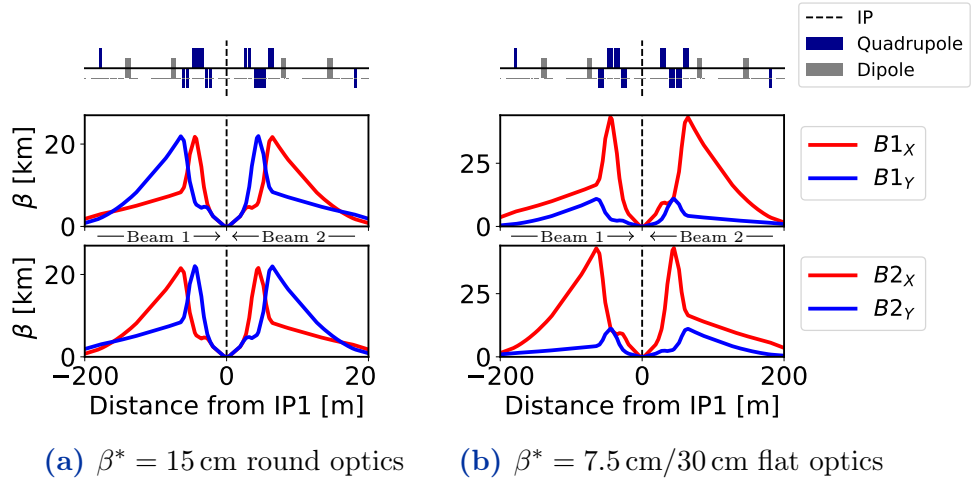
Figure 3: HL-LHC β-functions in the IR around IP1.

In the original implementation of the algorithm in [11], the optics of only one beam could be given and the algorithm was making use of the symmetries of the β-function in the IR

$$
\beta_x^{(B1)}(s) = \beta_y^{(B2)}(s)
$$
$$
\beta_y^{(B1)}(s) = \beta_x^{(B2)}(s) ,
$$

(15)

which is true for round optics as shown in Fig. 3a, to calculate a correction valid for both beams. With this symmetry the effective RDT Eq. (9) simply switches the β exponents between the beams, for which we will use the notation

$$
f_{jklm*}^{\text{IR (B1)}} \overset{Eq.\ (9)}{=} \int_{\text{IR}} \Re \left[i^{l+m} \left(K_n(s) + i J_n(s) \right) \right] \beta_x(s)^{\frac{l+m}{2}} \beta_y(s)^{\frac{j+k}{2}} e^{i\pi n\theta(s-s_{\text{IP}})} ds \overset{Eq.\ (15)}{=} f_{\text{lmjk}}^{\text{IR (B2)}} .
$$

(16)

As mentioned in the previous section, with the two correctors per field type (order and orientation), we can perfectly correct two RDTs locally in the IR. When

$$j + k \equiv l + m \quad \mod 2 \, , \tag{17}$$

i.e. both f_{jklm} and f_{lmjk} are skew (normal) RDTs, two RDTs per beam can be corrected: $f_{jklm*}^{\text{IR}} = \pm f_{lmjk}^{\text{IR}}$ within the optics of the same beam and we can therefore choose $f_{j'k'l'm'}^{\text{IR}} = f_{lmjk}^{\text{IR}}(= \pm f_{jklm*}^{\text{IR}})$ in Eq. (14). If on the other hand $j + k$ and $l + m$ are of different parity, only **one** RDT f_{jklm}^{IR} per beam can be corrected, by targeting f_{jklm}^{IR} and $f_{j'k'l'm'}^{\text{IR}} = f_{jklm*}^{\text{IR}}$ in the given optics.

There are optics in which Eq. (15) does not hold true anymore. For example, in contrast to *round* optics, in which the β-function at the IP ($\beta^* = \beta(s_{\text{IP}})$) is equal for both transversal planes ($\beta_x^* = \beta_y^*$), there exists also so called *flat* optics, for which $\beta_x^* \neq \beta_y^*$ (i.e. the beam shape is *flat* at the IP) [21, 22]. A realization of flat optics, forseen to be used in the HL-LHC, is shown in Fig. 3b.

The straightforward way to not to rely on Eq. (15), is to use the optics for both beams in the correction and construct Eq. (14) from both

$$\begin{pmatrix} b_{jklm}^{(cl,\text{B1})} & b_{jklm}^{(cr,\text{B1})} \\ b_{jklm}^{(cl,\text{B2})} & b_{jklm}^{(cr,\text{B2})} \end{pmatrix} \begin{pmatrix} K_n L_{cl} \\ K_n L_{cr} \end{pmatrix} = - \begin{pmatrix} I_{jklm}^{(\text{B1})} \\ I_{jklm}^{(\text{B2})} \end{pmatrix} \, . \tag{18}$$

2.3.3 Feed-Down

The effect of feed-down occurs whenever a particle beam is passing off-center through a magnet, due to either a transverse misalignment of the magnet or an off-center closed orbit of the beam itself. In these cases, the magnetic field can be described via Taylor expansion as a composition of magnetic field components with identical geometry as lower order fields in addition to the current field of higher order. These components therefore cause the same effects on the beam as lower order sources would [39].

Feed-down can be understood by applying a first-order Taylor Expansion $x \mapsto x + \Delta x$

and $y \mapsto y + \Delta y$ to Eq. (4) in the curvilinear (comoving) coordinate system

$$
\begin{aligned}
h = \quad & -\Re \left[\sum_{n=2}^{\infty} (K_n + iJ_n) \frac{(x+iy)^n}{n!} \right] \\
\overset{Taylor}{=} \quad & -\Re \left[\sum_{n=2}^{\infty} (K_n + iJ_n) \frac{\sum_{q=0}^{n} \frac{1}{q!} \frac{n!}{(n-q)!} (x+iy)^{n-q}(\Delta x + i\Delta y)^q}{n!} \right] \\
= \quad & -\Re \left[\sum_{n=2}^{\infty} (K_n + iJ_n) \sum_{q=0}^{n} \frac{(x+iy)^{n-q}(\Delta x + i\Delta y)^q}{q!\,(n-q!)} \right] \\
\overset{\substack{\text{sort by } (x+iy)^n \\ n \mapsto n+q}}{=} \quad & -\Re \left[\sum_{n=0}^{\infty} \sum_{\substack{q=0 \text{ if } n\geq 2 \\ q=2 \text{ if } n<2}}^{\infty} \frac{1}{q!\,n!} (K_{n+q} + iJ_{n+q})(x+iy)^n(\Delta x + i\Delta y)^q \right] \\
= \quad & -\Re \left[\sum_{n=0}^{\infty} \left(\sum_{\substack{q=0 \text{ if } n\geq 2 \\ q=2 \text{ if } n<2}}^{\infty} (K_{n+q} + iJ_{n+q}) \frac{(\Delta x + i\Delta y)^q}{q!} \right) \frac{(x+iy)^n}{n!} \right]
\end{aligned}
\tag{19}
$$

For brevity (s) is omitted, but h, K_n, J_n, x, y and $\Delta x, \Delta y$ are all dependent on the longitudinal location. From Eq. (19) one can see that magnetic field strengths of order $n \geq 2$ without feed-down are replaced by a sum depending on the deviation of the beam from magnet-center and higher order field strengths. Feed-down to field order $n \geq 2$ from fields up to $n + Q$ can now be calculated by:

$$
K_n + iJ_n \overset{\text{w/ feeddown}}{\to} \sum_{q=0}^{Q} (K_{n+q} + iJ_{n+q}) \frac{(\Delta x + i\Delta y)^q}{q!}. \tag{20}
$$

Fields feed-down can also have an effect on the scalar field ($n = 0$) and dipole fields ($n = 1$). As their structure does not follow the structure in Eq. (4), Eq. (20) is not applicable. In the context of RDTs n is always larger than 2 and we can use Eq. (20) in the definition of the effective RDT Eq. (9)

$$
f_{jklm}^{\text{IR}} = \int_{\text{IR}} \Re \left[i^{l+m} \sum_{q=0}^{\infty} (K_{n+q}(s) + iJ_{n+q}(s)) \frac{(\Delta x(s) + i\Delta y(s))^q}{q!} \right] \beta_x(s)^{\frac{j+k}{2}} \beta_y(s)^{\frac{l+m}{2}} e^{i\pi n\theta(s-s_{\text{IP}})} \mathrm{d}s , \tag{21}
$$

and can therefore easily include it when building the equation systems Eq. (13), Eq. (14) or Eq. (18).

Not only can feed-down be used to calculate the influence of field errors of orders $\geq n$ on the RDT, i.e. by contributing to the integral I_{jklm}, but it can also be used to calculate the strengths of correctors of orders $n_{\text{Corrector}} > n$ to counteract the RDT via feed-down. The matrix elements of the corrector coefficients in Eq. (12) will then also contain the feed-down coefficient

$$
z_p = \frac{(\Delta x + i\Delta y)^p}{p!} \tag{22}
$$

10

with p being the order of feed-down necessary, i.e.

$$p = n_{\text{Corrector}} - n \,. \tag{23}$$

As $z_p \in \mathbb{C}$, this makes the evaluation of the real part in Eq. (11), needed to split the equation system into two, separating the correctors (Eq. (13)), less straightforward and more cases need to be considered. Inserting

$$\Re\left[i^{l+m}(K_{n+p}L_w + iJ_{n+p}L_w)\frac{(\Delta x L_w + i\Delta y L_w)^q}{q!}\right]$$

$$\overset{Eq. \ (22)}{=} \Re\left[i^{l+m}(K_{n+p}L_w + iJ_{n+p}L_w) \cdot z_p\right] \tag{24}$$

$$= \Re\left[i^{l+m}(K_{n+p}L_w + iJ_{n+p}L_w)(\Re[z_p] + i\Im[z_p])\right]$$

$$= \Re\left[i^{l+m}\left[(K_{n+p}L_w \cdot \Re[z_p] - J_{n+p}L_w \cdot \Im[z_p]) + i(K_{n+p}L_w \cdot \Im[z_p] + J_{n+p} \cdot \Re[z_p])\right]\right]$$

into Eq. (11) yields the equation system

$$\left(\Re[z_p] \cdot b_{jklm}^{(cl)} \quad \Re[z_p] \cdot b_{jklm}^{(cr)} \quad -\Im[z_p] \cdot b_{jklm}^{(cl)} \quad -\Im[z_p] \cdot b_{jklm}^{(cr)}\right)\begin{pmatrix} K_{n+p}L_{cl} \\ K_{n+p}L_{cr} \\ J_{n+p}L_{cl} \\ J_{n+p}L_{cr} \end{pmatrix} = -I_{jklm} \quad \text{for even } l+m,$$

$$\left(i\,\Im[z_p] \cdot b_{jklm}^{(cl)} \quad i\,\Im[z_p] \cdot b_{jklm}^{(cr)} \quad i\,\Re[z_p] \cdot b_{jklm}^{(cl)} \quad i\,\Re[z_p] \cdot b_{jklm}^{(cr)}\right)\begin{pmatrix} K_{n+p}L_{cl} \\ K_{n+p}L_{cr} \\ J_{n+p}L_{cl} \\ J_{n+p}L_{cr} \end{pmatrix} = -I_{jklm} \quad \text{for odd } l+m \,.$$

$$\tag{25}$$

In the case of $p=0$, Eq. (25) transforms back to Eq. (13), as $\Re[z_0] = 1$ and $\Im[z_0] = 0$. For simplicity, we can redefine b_{jklm} to include the additional factors directly into the coefficients

$$b_{jklm,p} = \begin{cases} \Re[z_p] \cdot b_{jklm} & \text{if normal corrector and } l+m \text{ even,} \\ \Im[z_p] \cdot b_{jklm} & \text{if normal corrector and } l+m \text{ odd,} \\ -\Im[z_p] \cdot b_{jklm} & \text{if skew corrector and } l+m \text{ even,} \\ \Re[z_p] \cdot b_{jklm} & \text{if skew corrector and } l+m \text{ odd} \end{cases} \tag{26}$$

and take care to take z_p into account, whenever $p > 0$.

Including feed-down into the equation system also allows therefore to correct multiple orders of RDTs with the same correctors, as well as correcting RDTs with correctors of multiple orders. Equation (13) can hence not only be extended "vertically" by correcting for multiple beam optics (Eq. (18)) and different RDTs (Eq. (14)) at the same time, but also "horizontally", by adding more correctors, e.g.

$$\begin{pmatrix} b_{jklm}^{(cl)} & b_{jklm}^{(cr)} & b_{jklm,p}^{(cl)} & b_{jklm,p}^{(cr)} \\ b_{j'k'l'm'}^{(cl)} & b_{j'k'l'm'}^{(cr)} & b_{j'k'l'm',p}^{(cl)} & b_{j'k'l'm',p}^{(cr)} \end{pmatrix}\begin{pmatrix} K_n L_{cl} \\ K_n L_{cr} \\ K_{n+p}L_{cl} \\ K_{n+p}L_{cr} \end{pmatrix} = -\begin{pmatrix} I_{jklm} \\ I_{j'k'l'm'} \end{pmatrix} \tag{27}$$

3 Implementation

This chapter describes the implementation of the correction algorithm as realized in Version 1.0.0 of [25]. Direct links to lines of the code as well as usage of `python` is avoided, yet the structure and naming of the sections in this chapter follows is kept close to the names in the actual code, which can be found on https://github.com/pylhc/irnl_rdt_correction. The API is documented in https://pylhc.github.io/irnl_rdt_correction.

> **ATTENTION** While this note follows the convention of **n = 1 for dipole fields**, in the code the `MAD-X` convention of **n = 0 for dipole fields** is used, as the input will already be in that format.

DEPENDENCIES

The package is mostly self-contained and depends only on:

`numpy:` provides an easy way to work with numerical data in arrays as well as additional functionality e.g. for solving linear equation systems [40].

`pandas:` allows working with data-tables, which are used to structure the data and allow easy access and identification of the different optics parameters [41].

`tfs-pandas:` a wrapper for `pandas` to read tables from and write tables into files of the Table File System (TFS) format used by `MAD-X` [38] [42].

3.1 Beam Directions

(a) In reference frame of Beam 1   (b) In reference frame of Beam 2
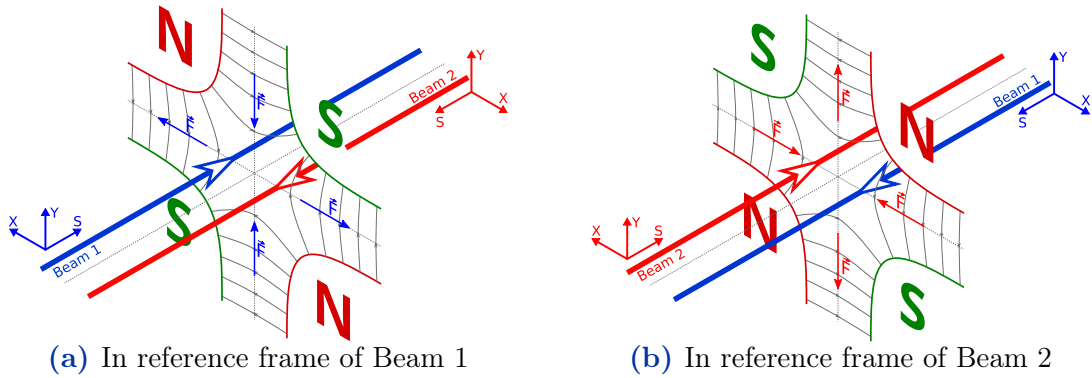
Figure 4: Schematic of two beams traveling in opposite directions through a quadruople.

Because of the opposite traveling direction of Beam 2, magnetic fields in the reference frame of this beam look as if rotated by 180° around the y-axis at the center of the magnet, compared to the reference frame of Beam 1. Hence magnets with y-axis symmetry will have the same effect on the beams, while magnets that do not have this symmetry will look like they have opposite-sign fields, e.g. a focusing quadrupole magnet with strength K_2 in Beam 1 is seen as a defocusing magnet with $-K_2$ in Beam 2 (see Fig. 4). In general:

$$(K_n + iJ_n)^{\text{B2}} = \begin{cases} (-K_n + iJ_n)^{\text{B1}} \text{, if } n \text{ is even} \\ (K_n - iJ_n)^{\text{B1}} \text{, if } n \text{ is odd .} \end{cases} \tag{28}$$

This does not need to be taken into account as long as one stays within the reference frame of a single beam, as the physics (e.g. feed-down and RDTs) is symmetrical. It becomes problematic when both beams are involved, especially as there are two different definitions for Beam 2 in `MAD-X`: One called is "Beam 2", for which all elements are defined in the reference frame of Beam 1 and the beam direction is handled via a negative beam velocity (`BV=-1`); the other one is called "Beam 4" and here the whole lattice is inverted and the beam travels in forward direction (`BV=1`), which means the field strengths follow the relation in Eq. (28). Of further confusion is the fact, that the beam direction is already taken into account in the field strength data of `TWISS` in `MAD-X`, but not in the `errors` output of `ESAVE` and not in the horizontal orbit, the `X` and `DX` data respectively. To assure consistent behaviour, the optics of "Beam 2" are brought into the reference frame of "Beam 4" upon loading.

When building an equation system as in Eq. (18), the reference frame needs again to be taken into account: Equation (18) is only correct, when all values are calculated in the same reference frame. Yet they are not. Each line of is correct in its own reference frame, but the K_nL and J_nL values are shared in between them. To account for the appropriate signs, the signs of the coefficients are inverted according to Eq. (28) where needed for Beam 2:

$$
\begin{pmatrix} b_{jklm}^{(cl,\text{B1})} & b_{jklm}^{(cr,\text{B1})} \\ \pm b_{jklm}^{(cl,\text{B2})} & \pm b_{jklm}^{(cr,\text{B2})} \end{pmatrix} \begin{pmatrix} K_nL_{cl} \\ K_nL_{cr} \end{pmatrix} = - \begin{pmatrix} I_{jklm}^{(\text{B1})} \\ I_{jklm}^{(\text{B2})} \end{pmatrix} \quad \text{if } n \text{ is } \{ \substack{\text{odd} \\ \text{even}} \, ,
$$
$$
\begin{pmatrix} ib_{jklm}^{(cl,\text{B1})} & ib_{jklm}^{(cr,\text{B1})} \\ \pm ib_{jklm}^{(cl,\text{B2})} & \pm ib_{jklm}^{(cr,\text{B2})} \end{pmatrix} \begin{pmatrix} J_nL_{cl} \\ J_nL_{cr} \end{pmatrix} = - \begin{pmatrix} I_{jklm}^{(\text{B1})} \\ I_{jklm}^{(\text{B2})} \end{pmatrix} \quad \text{if } n \text{ is } \{ \substack{\text{even} \\ \text{odd}} \, .
$$
$$(29)$$

Calculating the corrector strengths in this way also allows for easy setting of the `MAD-X` knobs to set the corrector strengths, as these are defined with positive sign in the lattice sequence of Beam 1 (and "Beam 2") and negative sign in the lattice sequence of "Beam 4". On the other hand, when updating the optics tables itself, e.g. to correct feed-down from the correctors, the original signs need to be recovered for "Beam 2" and "Beam 4".

This is the way the beam direction is currently implemented in the code. Where this sign change is applied, it will be explicitly mentioned again in the following chapters.

> HINT Another option would be to bring everything into the reference frame of Beam 1 in the first place, i.e. switching the signs of the "Beam 4" K_nL and J_nL according to Eq. (28), in `twiss` and `errors`, as well as the same K_nL, J_nL in the `twiss` of "Beam 2". It still needs to be shown, that in this case feed-down is correctly calculated, as the direction of the beam is no longer taken into consideration. If this is shown, all beam related sign changes in the code, but the initial one to bring as described just now upon loading `twiss` and `errors`, could be removed. See also Section 3.4.

3.2 Main

The entry-point to run the corrections is the `irnl_rdt_correction()` function in `irnl_rdt_correction/main.py`.

3.2.1 Preparations

CHECK OPTS

First the `options` given by the user are validated and default values set. These options are:

twiss: the optics of the machine as given by the `TWISS` command in `MAD-X`. **Important:** All of these elements are used for correction. They are assumed to follow the LHC naming scheme, so that they can be split into IRs, but to limit the correction to only calculate the effective RDT over certain IR elements, these need to be filtered **beforehand**, e.g. in `MAD-X`.

errors: errors on the optics of the machine, as given by the `ESAVE` command in `MAD-X`. All elements of errors need to be present in twiss, but elements not present in errors are assumed to have zero errors.

beam: the beam the optics come from, definition as in `MAD-X`: 1, 2 or 4.

output: path to write the results into (as table and as `MAD-X` commands.)

rdts: a set of RDTs, defined either like f_{jklm} (f_{jklm*}) as strings of format `"fjklm"` (`"fjklm*"`) to correct these RDTs (RDTs with switched β, see Eq. (16)) by the correctors of their order and orientation. Alternatively they can be given as a dictionary, with the RDTs as keys and a list of corrector fields (e.g. b_4) as strings (e.g. `"b4"`) as values to specify which correctors to use to correct this RDT Eq. (13). If the order of the corrector is higher than the order of the RDT, its feed-down is used to correct the RDT. If the order is lower, an error is raised. If rdts2 is given, these apply only `MAD-X` to the first optics. (Default depends on accel)

rdts2: same format as rdts, but the given RDTs are used to correct the second optics. If only rdts is given, they apply to all optics.

accel: The name of the accelerator to use. `"lhc"` and `"hllhc"` are implemented. This determines the default RDTs to use, as well as the correct names for the correctors in the lattice. (Default: `"lhc"`)

feeddown: maximum order of the feed-down to include, i.e. Q in Eq. (20).

ips: a list of integers of the IPs to correct. (Default: 1,2,5,8)

solver: solver to use to solve the built linear equation system. Can be one of `"lstsq"`, `"inv"` or `"linear"`. (Default `"lstsq"`).

update_optics: if this option is set to `True`, the correction begins with the highest order and the newly calculated corrector strengths are inserted into the optics for the following so that feed-down from these correctors can be taken into account. Necessary for accurate corrections in case $Q \geq 0$ (as set via feeddown). (Default: `True`)

ignore_corrector_settings: if this is `False`, the corrector values of the optics are used as initial conditions. Otherwise they are ignored. (Default: `False`)

ignore_missing_columns: if `True` missing strength columns in any of the input files are assumed to be zero, instead of raising an error. (Default: `False`)

iterations: (re-)iterate correction, starting with the previously calculated values. Needs to be > 0, as the first calculation counts as an iteration. (Default: 1)

The default RDTs for the LHC and HL-LHC are as in the original triplet correction scripts [43, 44]:

Table 1: Default RDTs used in the correction script if `rdts` option is not provided.

accel	RDTs		description
`"lhc"`	`"F0003"`	`"F0003*"`	correct a_3 errors with f_{0003}
	`"F1002"`	`"F1002*"`	correct b_3 errors with f_{1002}
	`"F1003"`	`"F3001"`	correct a_4 errors with f_{1003} and f_{3001}
	`"F4000"`	`"F0004"`	correct b_4 errors with f_{4000} and f_{0004}
	`"F6000"`	`"F0006"`	correct b_6 errors with f_{6000} and f_{0006}
`"hllhc"`	`"F0003"`	`"F0003*"`	correct a_3 errors with f_{0003}
	`"F1002"`	`"F1002*"`	correct b_3 errors with f_{1002}
	`"F1003"`	`"F3001"`	correct a_4 errors with f_{1003} and f_{3001}
	`"F0004"`	`"F4000"`	correct b_4 errors with f_{0004} and f_{4000}
	`"F0005"`	`"F0005*"`	correct a_5 errors with f_{0005}
	`"F5000"`	`"F5000*"`	correct b_5 errors with f_{5000}
	`"F5001"`	`"F1005"`	correct a_6 errors with f_{5001} and f_{1005}
	`"F6000"`	`"F0006"`	correct b_6 errors with f_{6000} and f_{0006}

SORT RDTs

The input RDTs are then transformed into `RDT`-objects, which contain information about their order $n = j + k + l + m$, their skewness ($l + m \equiv 1 \mod 2$) and wether they should be calculated with swapped β-exponents (if given by the $*$ in the name). A mapping is then produced to the desired correctors these RDTs should be corrected with, resulting in a dictionary of `RDT`-objects and sequences of strings, defining corrector orientation and order (e.g. `"b4"`). The latter are either taken from the user input parameters, or if not given, determined by the RDT itself. This mapping is then sorted by highest RDT order and (arbitrarily) skew before normal.

GET ORDERS

Now, the feed-down orders are checked. It is for example not possible to update the optics in a useful manner, if two orders of feed-down are required and a normal octupole RDT (b_4) should be corrected by feed-down from a normal dodecapole corrector (b_6), while at the same time a normal decapole RDT (b_5) needs to be corrected by a corrector of the same order. As the b_5 RDT is corrected before the b_4 RDT, the b_6 corrector is still unassigned and its

feed-down cannot be taken into account when calculating the b_5 correction. This issue could be overcome by sorting not by highest RDT order but by highest corrector order per RDT, which is implemented but has yet to be tested (see Section 3.4).

It is also checked, wether the field order of a given corrector is lower than the order of its RDT, as in this case the corrector can have no influence on the effective RDT (as they are RDTs of first order in field strengths). In this case an error is thrown.

Also the `needed orders` are evaluated, which are the field orders needed in the optics to calculate all desired effective RDTs with the requested `feeddown`.

Load Optics

If the `twiss` and `errors` are not given as TfsDataFrames already, they are then read in. It is checked that the number of `twiss` and `errors` tables given equals. The contents of the tables themselves are checked for the presence of elements, e.g. elements in `errors` need to be present in `twiss`, as their position and β-functions need to be known. Elements not found in `errors`, which are present in `twiss` are added with zero values. It is then also checked if all `needed orders` as determined in the previous step are present in the KNL and KNSL columns of the `TfsDataFrames`. Depending on the choice of `ignore_missing_columns` they are either filled with zeros or the program ends with an error.

At this point, the beam direction is also taken care of, i.e. if `twiss` and `errors` of MAD-X' "Beam 2" are given, the horizontal orbit columns in both (`X` and `DX`) will switch sign, as well as all strengths of magnets, that are not symmetric on beam direction change, or *anti mirror-symmetric* as it is called in the code. In this manner, the optics of "Beam 2" are brought into the reference frame of "Beam 4". See Section 3.1 for details.

For convenience, the loaded optics are then stored in a sequence of `Optics`-objects, each containing single instance of the given `beam`, `twiss` and `errors`.

3.2.2   Build and Solve Equation System

The core of the correction algorithm is the building and solving of the equation system Eq. (13) and extending it for multiple RDTs (Eq. (14)), beam optics (Eq. (18) and Eq. (29)), but also possibly solving for multiple correctors at a time when correcting via feed-down (Eq. (25)).

Get RDT Maps grouped by Correctors

To increase numerical stability and also allow to incorporate feed-down from correctors to lower order RDTs, not all corrector strengths are calculated at the same time, but many independent equation systems are build, and solved consecutively.

To achieve this, the RDTs to correct are grouped by common correctors: The correctors of the first RDT, as given by the built RDT map in **Sort RDTs** in Section 3.2.1, are used to find other RDTs sharing these correctors, the correctors of which are then used to determine which other RDTs need to be corrected together, until all remaining RDTs have no correctors in common with the selected ones. The grouping is done for all given optics at the same go, so that also common correctors are found between them.

After solving the equation system for the currently selected RDTs, the process of grouping RDTs is repeated with the remaining RDTs until none are left. As this algorithm for grouping is not straightforward, details about the actual implementation are found directly in the comments of the code.

Get available Correctors

In a loop over the given `ips`, the so far abstract corrector names, identifying only orientation and order of the correctors, are now instancialized as `Corrector`-objects by finding the appropriate correctors for the current IP in the `Optics`. The current implementation is very (HL-)LHC specific, as it uses the naming scheme, depending on the given `accel`. If correctors are present in only one of the given `Optics`, but not in the other, an `EnvironmentError` is raised. When only one of the two correctors per side is present, a `warning` is printed, and if no matching corrector for this IP is found in the optics, this `information` is logged and the corrector not included in the correction of this IP.

The corrector values are initialized in accordance with `ignore_corrector_settings` (they are initialized as zero, or as given in the optics) and saved in case they need to be restored later (`update_optics = False`). This is important, as the algorithm actually calculates the *change in corrector strength* needed to compensate the RDT, as explained in the next paragraph.

Build Equation System

The equation system for the current RDTs, correctors and optics including the desired feed-down (Eqs. (13), (14), (18), (25) and (29)) for the current IP, e.g.

$$
\begin{pmatrix}
b_{jklm}^{(cl,\text{IP1,B1})} & b_{jklm}^{(cr,\text{IP1,B1})} & b_{jklm,p}^{(cl,\text{IP1,B1})} & b_{jklm,p}^{(cr,\text{IP1,B1})} & \cdots \\
b_{jklm}^{(cl,\text{IP1,B2})} & b_{jklm}^{(cr,\text{IP1,B2})} & b_{jklm,p}^{(cl,\text{IP1,B2})} & b_{jklm,p}^{(cr,\text{IP1,B2})} & \cdots \\
b_{j'k'l'm'}^{(cl,\text{IP1,B1})} & b_{j'k'l'm'}^{(cr,\text{IP1,B1})} & b_{j'k'l'm',p}^{(cl,\text{IP1,B1})} & b_{j'k'l'm',p}^{(cr,\text{IP1,B1})} & \cdots
\end{pmatrix}
\begin{pmatrix}
\Delta K_n L_{cl} \\
\Delta K_n L_{cr} \\
\Delta K_{n+p} L_{cl} \\
\Delta K_{n+p} L_{cr} \\
\vdots
\end{pmatrix}
= -
\begin{pmatrix}
I_{jklm}^{(\text{IP1,B1})} \\
I_{jklm}^{(\text{IP1,B2})} \\
I_{j'k'l'm'}^{(\text{IP1,B1})} \\
\vdots
\end{pmatrix}, \quad (30)
$$

is now build. In contrast to Eq. (11), the integrals I_{jkml} on the rhs of Eq. (30) contain also the corrector settings as currently in the `Optics`. For this reason, the $\Delta K_n L$ values are introduced here, which allow to solve and update this equation system as often as given in `iterations` to improve upon in a next step.

Special care is taken to swap the β-exponent in the integral as well as in the coefficients b_{jklm}, in case f_{jklm*} is given. In accordance with the implementation of the LHC and HL-LHC Sequences in `MAD-X`, also the sign of b_{jklm} might be inversed for Beam 2 and Beam 4, depending on the symmetry of the magnet (see Section 3.1).

Solve Equation System and update Values

The built linear equation system is now solved with one of the standard solvers, as given by via the option `solver`. `"inv"` and `"linear"` refer hereby to inverting the coefficient matrix on the lhs of Eq. (30) and performing a dot-product with the rhs and to solving it directly via `numpy`'s `solve` method, respectively. These are only implemented for testing and

debugging purposes and should not be used in real applications as they are inefficient and work only with well-determined matrix equations. The default method `"lstsq"` makes use of the `numpy` method of the same name and performs a linear least-squares optimization and works on under-, well-, or over-determined equation systems.

As explained above the resulting values are the changes to the current corrector values, which are now applied and used to update the optics and the integrals on the rhs of Eq. (30) are recalculated, informing about the change in the effective RDTs and to be used in the next `iteration`, if there will be one.

After the `iteration`s for the current IP have been run, the original corrector values will be restored, if they had been saved (see **Get available Correctors**) and the corrections for the next given IP is calculated.

Output

After all corrector values have been calculated, they are finally written into `ASCII`-files, if `outpath` is given, and returned in two different formats:

As `MAD-X` In this format the corrector names are converted into the circuit-knob-names as used in the lattice description in `MAD-X`. As these refer to the non-integrated field strengths, the value is assigned by reference (`:=`) and divided by the lattice variable for the length of the corrector type (e.g. `l.MCTX`). In this format, the correction can be immediately used in a `MAD-X` script.

As `TfsDataFrame` The second output format is a `DataFrame`, created from `IRCorrector`-objects. The attributes are mapped to the columns, while the different correctors are spread along the index. The `DataFrame` is written out as a table in `TFS` format by `tfs-pandas`.

3.3 Tests

A variety of tests has been deployed, testing the current status of the current implementation and trying to make the algorithm resilient against future bugs. The tests are automatically run via github workflows and need to pass before any pull-request is accepted to the "master"-branch of the repository.

Most tests cover certain specific ways to run the correction algorithm as a whole, while also some unit-tests have been implemented, where easily applicable. To be able to validate the calculated corrections easily a non-physical `pseudo-model` is created in most tests, with only a few of elements and arbitrary values for the parameters. For example, a constant β-function of 1 can be used to simplify the equation systems and make them solvable by hand. Currently running are tests for the following scenarios:

Standard Corrections Test default correction capabilities.

    Basic Test the basic correction functionality and perform some sanity checks. Operates on a pseudo-model so that the corrector values are easily known. Sanity Checks:
- all correctors found

- corrects have the correct value (as set by errors or zero)
- all corrector circuits are present in the `MAD-X` script

LHC Correction Test LHC optics with random errors assigned. Sanity Checks:
- all correctors found
- correctors have a value
- all corrector circuits are present in the `MAD-X` script

RDT CORRECTIONS Test correction settings that are RDT specific.

Different RDTs Test that different RDTs can be corrected and only their correctors are returned. Also checks that the corrector values are varying between RDTs when they should. Octupole RDTs are used for this example.

Switched Beta Test using the special RDTs* where the beta-exponents are switched.

DUAL OPTICS CORRECTIONS Test the correction when giving more than one beam optics.

Dual Optics Test that given two different optics an approximate solution will be found.

Dual Optics RDTs Test calculations given two different optics and different RDTs.

FEED-DOWN CORRECTIONS Test the feed-down calculation and correction.

General Test feed-down functionality from decapoles to octupoles and sextupoles.

Correct via Feed-Down Test correct RDT via feed-down from higher order corrector: Use normal and skew deca- and dodecapole correctors to correct for octupole errors.

UNIT-TESTS Test individual functions and classes.

Switch Signs Test the sign-switching function from Beam 2 to Beam 4 (and that there is no switch given Beam 1 or Beam 4).

IRCorrector Class Test the class representing IR Correctors
- instantiates
- has the right (in-)equalities
- is sortable
- for different accelerators

RDT Class Test the class representing RDTs
- instantiates
- has the right (in-)equalities
- is sortable

3.4   To Do

EASY Allow not giving errors (need to be `None` in the list or all `None`, so that the list lengths are still the same and there is a clear correspondence twiss-errors-beams). They should then be assumed all zero.

EASY Allow for more than two optics given (e.g. find corrections for 15cm and 30cm for both beams).

MEDIUM Maybe sort RDTs by highest corrector instead of highest RDT order? This should allow for correctors that correct via feed-down to be assigned before lower order RDTs are calculated. It is already in the code, but commented out for now as might cause other problems. To be thought about and tested. See GET ORDERS in Section 3.2.1.

MEDIUM Consider switching the signs all into the reference frame of Beam 1. That means X, DX and anti-mirror-KN(S)L twiss and errors from Beam 4, and the anti-mirror-KN(S)L twiss from Beam 2. That should in principle allow to ignore all other beam-related sign switches. BUT: does this really work with all the feed-down options implemented (i.e. feed-down to RDT, feed-down from correctors)? It should, but needs to be checked and tested. See HINT in Section 3.1.

MEDIUM Take phase advance between the elements and to the correction point at the entrance of the IR into account. That would mean correct the numerator of the *actual* RDT (Eq. (7)) instead of the *effective* RDT (Eq. (9)).

HARD Additionally to taking the phase-advance into account, one might try to optimize the actual RDTs at the position of the correctors. This might be very problematic, as we have two correctors (one on each side) per order, so that might become a non-linear problem (as now there are now two equations, one per corrector, which are non-linearly dependent.)

4 Applications

The new correction package has already been extensively used for studies of the LHC and HL-LHC optics. The influence of feed-down has been studied in [45], while the correctability of asymmetric optics has been investigated in [46]. In another study, the feasibility to correct systematic normal decapole errors in the separation and recombination dipoles of the HL-LHC [47, 48] has been tested. The ease of use and availability allows to utilize the new package with little effort in future studies of non-linear IR corrections.

The algorithm has been received with interest and additional features have been suggested. Among these is the inclusion of the phase-advance between elements, to further approach (and correct) the exact value of the RDT, instead of the *effective* RDTs targeted in the current implementation, which has already been inlcuded into the *"To Do"* of Section 3.4 in this note.

5 Conclusion

An improved algorithm to correct nonlinear errors by locally compensating effective RDTs in the IRs has been derived and implemented, overcoming the rigidness of previous implementations and giving the user more control over the correction. Its main features include the option to target arbitrary RDTs, include more than one beam optics, and either include

feed-down into the RDTs to be corrected, or using the feed-down from the corrector magnets themselves for compensation.

This note is meant to be a supplement documentation to the code found at [25] changes in this pdf should be reflected in the repository and vice-versa.

References

[1] E. H. MACLEAN, F. S. CARLIER, AND J. COELLO DE PORTUGAL, *Commissioning of Non-linear Optics in the LHC at Injection Energy*, in Proceedings of IPAC, Busan, Korea, 2016, p. 4. URL: `https://cds.cern.ch/record/2207446`, `doi:10.18429/JACoW-IPAC2016-THPMR039`.

[2] E. H. MACLEAN, F. CARLIER, J. M. COELLO DE PORTUGAL, A. GARCIA-TABARES, M. GIOVANNOZZI, L. MALINA, T. PERSSON, P. SKOWROŃSKI, AND R. TOMÁS, *New Methods for Measurement of Nonlinear Errors in LHC Experimental IRs and Their Application in the HL-LHC*, in IPAC2017, Copenhagen, Denmark, 2017. URL: `https://cds.cern.ch/record/2289663`, `doi:10.18429/JACoW-IPAC2017-WEPIK093`.

[3] E. H. MACLEAN, ET AL., *New LHC optics correction approaches in 2017*, Dec. 2017, p. 7. URL: `https://indico.cern.ch/event/663598/contributions/2781846`.

[4] E. H. MACLEAN, ET AL., *Detailed review of the LHC optics commissioning for the nonlinear era*, Accelerators & Technology Sector Note CERN-ACC-2019-0029, Feb. 2019. URL: `http://cds.cern.ch/record/2655741`.

[5] E. H. MACLEAN, ET AL., *New approach to LHC optics commissioning for the nonlinear era*, Phys. Rev. Accel. Beams **22** (2019), p. 061004. URL: `https://link.aps.org/doi/10.1103/PhysRevAccelBeams.22.061004`, `doi:10.1103/PhysRevAccelBeams.22.061004`.

[6] E. H. MACLEAN, F. CARLIER, J. DILLY, R. TOMÁS, AND M. GIOVANNOZZI, *Prospects for beam-based study of dodecapole nonlinearities in the CERN High-Luminosity Large Hadron Collider*, submitted (2022).

[7] N. SAMMUT, L. BOTTURA, AND J. MICALLEF, *Mathematical formulation to predict the harmonics of the superconducting Large Hadron Collider magnets*, Phys. Rev. ST Accel. Beams **9** (2006), p. 012402. URL: `https://link.aps.org/doi/10.1103/PhysRevSTAB.9.012402`, `doi:10.1103/PhysRevSTAB.9.012402`.

[8] N. J. SAMMUT, L. BOTTURA, P. BAUER, G. VELEV, T. PIELONI, AND J. MICALLEF, *Mathematical formulation to predict the harmonics of the superconducting Large Hadron Collider magnets. II. Dynamic field changes and scaling laws*, Phys. Rev. ST Accel. Beams **10** (2007), p. 082802. URL: `https://link.aps.org/doi/10.1103/PhysRevSTAB.10.082802`, `doi:10.1103/PhysRevSTAB.10.082802`.

[9] N. SAMMUT, L. BOTTURA, G. DEFERNE, AND W. V. DELSOLARO, *Mathematical formulation to predict the harmonics of the superconducting Large Hadron Collider magnets: III. Precycle ramp rate effects and magnet characterization*, Phys. Rev.

ST Accel. Beams **12** (2009), p. 102401. URL: `https://link.aps.org/doi/10.1103/PhysRevSTAB.12.102401`, `doi:10.1103/PhysRevSTAB.12.102401`.

[10] L. DENIAU, H. GROTE, G. ROY, AND F. SCHMIDT, *MAD-X User Guide.* URL: `http://cern.ch/madx/releases/last-rel/madxuguide.pdf`.

[11] O. S. BRÜNING, M. GIOVANNOZZI, S. D. FARTOUKH, AND T. RISSELADA, *Dynamic aperture studies for the LHC separation dipoles*, Tech. Rep. LHC Project Note 349, CERN, 2004. URL: `https://cds.cern.ch/record/742967`.

[12] E. H. MACLEAN, R. TOMÁS, M. GIOVANNOZZI, AND T. H. B. PERSSON, *First measurement and correction of nonlinear errors in the experimental insertions of the CERN Large Hadron Collider*, Phys.Rev. ST Accel.Beams **18** (2015), p. 121002. URL: `https://doi.org/10.1103/PhysRevSTAB.18.121002`, `doi:10.1103/PhysRevSTAB.18.121002`.

[13] R. TOMÁS, O. BRÜNING, M. GIOVANNOZZI, P. HAGEN, M. LAMONT, F. SCHMIDT, G. VANBAVINCKHOVE, M. AIBA, R. CALAGA, AND R. MIYAMOTO, *CERN Large Hadron Collider optics model, measurements, and corrections*, Phys. Rev. ST Accel. Beams **13** (2010), p. 121004. URL: `https://link.aps.org/doi/10.1103/PhysRevSTAB.13.121004`, `doi:10.1103/PhysRevSTAB.13.121004`.

[14] T. H. B. PERSSON, Y. INNTJORE LEVINSEN, R. TOMÁS, AND E. H. MACLEAN, *Chromatic coupling correction in the Large Hadron Collider*, Phys. Rev. ST Accel. Beams **16** (2013), p. 081003. URL: `https://doi.org/10.1103/PhysRevSTAB.16.081003`, `doi:10.1103/PhysRevSTAB.16.081003`.

[15] J. DILLY, *Amplitude Detuning from misaligned Triplets and IR multipolar Correctors*, WP2 Meeting, Feb. 2020. URL: `https://indico.cern.ch/event/878274/contributions/3699998/attachments/1989167/3315808/presentation.pdf`.

[16] S. FARTOUKH AND F. ZIMMERMANN, *The HL-LHC Accelerator Physics Challenges*, vol. 24, WORLD SCIENTIFIC, Oct. 2015, pp. 45–96. URL: `http://www.worldscientific.com/doi/abs/10.1142/9789814675475_0004`, `doi:10.1142/9789814675475_0004`.

[17] *High-Luminosity Large Hadron Collider (HL-LHC): Technical design report*, CERN Yellow Reports: Monographs CERN-2020-010, CERN, Geneva, 2020. URL: `https://cds.cern.ch/record/2749422`, `doi:10.23731/CYRM-2020-0010`.

[18] E. H. MACLEAN, ET AL., *Nonlinear optics commissioning in the LHC*, in Evian, 2016, p. 9. URL: `https://indico.cern.ch/event/578001/contributions/2366314/attachments/1374391/2158727/2016_EvianPaper.pdf`.

[19] E. H. MACLEAN, R. TOMAS GARCIA, T. H. B. PERSSON, AND F. S. CARLIER, *Report from LHC MD 2171: Amplitude dependent closest tune approach from normal and skew octupoles*, accelerators & Technology Sector Note, 2018. URL: `http://cds.cern.ch/record/2310163`.

[20] X. Buffat, et al., *Optics measurement and correction strategies for HL-LHC*, Accelerators & Technology Sector Note CERN-ACC-2022-0004, CERN, Apr. 2022. URL: `https://cds.cern.ch/record/2808650`.

[21] S. Fartoukh, *Achromatic telescopic squeezing scheme and application to the LHC and its luminosity upgrade*, Phys. Rev. ST Accel. Beams **16** (2013). `doi:10.1103/PhysRevSTAB.16.111002`.

[22] S. Fartoukh, N. Karastathis, L. Ponce, M. Solfaroli, and R. Tomas, *About flat telescopic optics for the future operation of the LHC*, Accelerators & Technology Sector Note CERN-ACC-2018-0018, June 2018. URL: `https://cds.cern.ch/record/2622595/`.

[23] S. Fartoukh, et al., *First High-Intensity Beam Tests with Telescopic Flat Optics at the LHC*, Accelerators & Technology Sector Note CERN-ACC-2019-0052, 2019. URL: `http://cds.cern.ch/record/2687343`.

[24] J. Dilly, *Correction of Amp det and RDTs for flat optics*, OMC-Meeting, CERN, July 2018. URL: `https://indico.cern.ch/event/742348/contributions/3069299/`.

[25] OMC-Team and J. Dilly, *IRNL RDT Correction*. CERN. URL: `https://github.com/pylhc/irnl_rdt_correction`, `doi:10.5281/zenodo.6373375`.

[26] R. De Maria, R. Bruce, D. Gamba, M. Giovannozzi, and F. Plassard, *High Luminosity LHC Optics and Layout HLLHCV1.4*, Journal of Physics: Conference Series **1350** (2019), p. 012001. `doi:10.1088/1742-6596/1350/1/012001`.

[27] R. De Maria, et al., *CERN Optics Repository*. URL: `https://acc-models.web.cern.ch/`.

[28] A. J. Dragt and J. M. Finn, *Lie series and invariant functions for analytic symplectic maps*, Journal of Mathematical Physics **17** (1976), pp. 2215–2227. URL: `https://aip.scitation.org/doi/10.1063/1.522868`, `doi:10.1063/1.522868`.

[29] A. J. Dragt, *Lie algebraic theory of geometrical optics and optical aberrations*, J. Opt. Soc. Am., JOSA **72** (1982), pp. 372–379. URL: `https://opg.optica.org/josa/abstract.cfm?uri=josa-72-3-372`, `doi:10.1364/JOSA.72.000372`.

[30] É. Forest, *A Hamiltonian-free description of single particle dynamics for hopelessly complex periodic systems*, Journal of Mathematical Physics **31** (1990), pp. 1133–1144. URL: `http://aip.scitation.org/doi/10.1063/1.528795`, `doi:10.1063/1.528795`.

[31] R. Tomás, *Direct Measurement of Resonance Driving Terms in the Super Proton Synchrotron (SPS) of CERN Using Beam Position Monitors*, PhD thesis, 2003. URL: `http://cds.cern.ch/record/615164`.

[32] E. D. Courant and H. S. Snyder, *Theory of the alternating-gradient synchrotron*, Annals of Physics **3** (1958), pp. 1–48. URL: `http://www.sciencedirect.com/science/article/pii/0003491658900125`, `doi:10.1016/0003-4916(58)90012-5`.

23

[33] A. FRANCHI, *Studies and Measurements of Linear Coupling and Nonlinearities in Hadron Circular Accelerators*, doctoral Thesis, Johann Wolfgang Goethe-Universität, Sept. 2006. URL: `https://publikationen.ub.uni-frankfurt.de/frontdoor/index/index/year/2006/docId/2270`.

[34] F. SCHMIDT, R. TOMÁS, AND A. FAUS-GOLFE, *Measurement of Driving Terms*, SPS and LHC Division Note CERN-SL-2001-039-AP, Chicago, 2001. URL: `http://cds.cern.ch/record/510665/`.

[35] R. TOMÁS, M. BAI, R. CALAGA, W. FISCHER, A. FRANCHI, AND G. RUMOLO, *Measurement of global and local resonance terms*, Phys. Rev. ST Accel. Beams **8** (2005). URL: `https://link.aps.org/doi/10.1103/PhysRevSTAB.8.024001`, `doi:10.1103/PhysRevSTAB.8.024001`.

[36] A. FRANCHI, L. FARVACQUE, F. EWALD, G. L. BEC, AND K. B. SCHEIDT, *First simultaneous measurement of sextupolar and octupolar resonance driving terms in a circular accelerator from turn-by-turn beam position monitors data*, Phys. Rev. Spec. Top. - Accel. Beams **17** (2014). `arXiv:1402.1461`, `doi:10.1103/PhysRevSTAB.17.074001`.

[37] F. S. CARLIER AND J. COELLO DE PORTUGAL, *Observations of Resonance Driving Terms in the LHC during Runs I and II*, 2016, p. 4. URL: `https://cds.cern.ch/record/2141782`.

[38] CERN - ACCELERATOR BEAM PHYSICS GROUP, *Methodical Accelerator Design - MAD*. URL: `http://madx.web.cern.ch/madx/`.

[39] H. WIEDEMANN, *Particle Accelerator Physics*, Graduate Texts in Physics, Springer International Publishing, Cham, fourth ed., 2015. URL: `http://link.springer.com/10.1007/978-3-319-18317-6`, `doi:10.1007/978-3-319-18317-6`.

[40] C. R. HARRIS, ET AL., *Array programming with NumPy*, Nature **585** (2020), pp. 357–362. URL: `https://www.nature.com/articles/s41586-020-2649-2`, `doi:10.1038/s41586-020-2649-2`.

[41] THE PANDAS DEVELOPMENT TEAM, *Pandas-dev/pandas: Pandas*. Zenodo. URL: `https://doi.org/10.5281/zenodo.3509134`, `doi:10.5281/zenodo.3509134`.

[42] OMC-TEAM, M. HOFER, J. DILLY, F. SOUBELET, L. MALINA, M. L. GARREC, J. M. C. DE PORTUGAL-MARTINEZ VAZQUEZ, R. TOMÁS, AND T. PERSSON, *TFS-Pandas*. CERN. URL: `https://github.com/pylhc/tfs`, `doi:10.5281/ZENODO.5070986`.

[43] S. FARTOUKH, *LHC nonlinear triplet and D1 correction script*, Sept. 2008. URL: `/afs/cern.ch/eng/lhc/optics/V6.503/toolkit/corr_tripD1`.

[44] S. FARTOUKH, *HL-LHC nonlinear triplet and D1 correction script*, 2012. URL: `/afs/cern.ch/eng/lhc/optics/HLLHCV1.4/errors/corr_tripD1_v6`.

[45] J. Dilly, E. H. Maclean, and R. Tomás, *Corrections of Feed-Down of Non-Linear Field Errors in LHC and HL-LHC Insertion Regions*, in IPAC2021, JACoW, June 2021, p. MOPAB259. `doi:10.18429/JACoW-IPAC2021-MOPAB259`.

[46] J. Dilly, E. H. Maclean, and R. Tomás, *Corrections of Non-Linear Field Errors With Asymmetric Optics in LHC and HL-LHC Insertion Regions*, in IPAC2021, JACoW, June 2021, p. MOPAB258. `doi:10.18429/JACoW-IPAC2021-MOPAB258`.

[47] J. Dilly, *Feasibility of correcting systematic b5 in D2*, 11th HL-LHC Collaboration Meeting, CERN, Oct. 2021. URL: `https://indico.cern.ch/event/1079026/contributions/4546005/`.

[48] J. Dilly, F. F. Van der Veken, M. Giovannozzi, and R. Tomás, *Correnctions of systematic normal decapole field errors in the HL-LHC separation/recombination dipoles*, in IPAC'22, This Conference, Bangkok, Thailand, 2022.

Appendices